Human Molecular Genetics, 2015, Vol. 24, No. 17 5060–5068

doi: 10.1093/hmg/ddv211
Advance Access Publication Date: 5 June 2015
Association Studies Article

ASSOCIATION STUDIES ARTICLE

WNT10A exonic variant increases the risk of keratoconus by decreasing corneal thickness

Gabriel Cuellar-Partida[1], Henriët Springelkamp[2,3], Sionne E. M. Lucas[5], Seyhan Yazar[7], Alex W. Hewitt[6,14], Adriana I. Iglesias[2,3], Grant W. Montgomery[12], Nicholas G. Martin[13], Craig E. Pennell[8], Elisabeth M. van Leeuwen[3], Virginie J. M. Verhoeven[2,3], Albert Hofman[3,9], André G. Uitterlinden[3,4,9], Wishal D. Ramdas[2], Roger. C. W. Wolfs[2], Johannes R. Vingerling[2,3], Matthew A. Brown[10], Richard A. Mills[11], Jamie E. Craig[11], Caroline C. W. Klaver[2,3], Cornelia M. van Duijn[3], Kathryn P. Burdon[5], Stuart MacGregor[1,*] and David A. Mackey[7]

[1]Statistical Genetics, QIMR Berghofer Medical Research Institute, Brisbane, Australia, [2]Department of Ophthalmology, [3]Department of Epidemiology, [4]Department of Internal Medicine, Erasmus Medical Center, Rotterdam 3000 CA, The Netherlands, [5]Menzies Institute for Medical Research, [6]School of Medicine, Menzies Research Institute Tasmania, University of Tasmania, Hobart, Australia, [7]Centre for Ophthalmology and Visual Science, Lions Eye Institute, University of Western Australia, [8]School of Women's and Infants' Health, University of Western Australia, Perth, Australia, [9]Netherlands Consortium for Healthy Ageing, Netherlands Genomics Initiative, the Hague 2593 CE, The Netherlands, [10]University of Queensland Diamantina Institute, Translational Research Institute, Princess Alexandra Hospital, Brisbane, Australia, [11]Department of Ophthalmology, Flinders University, Adelaide, SA, Australia, [12]Molecular Epidemiology, [13]Genetic Epidemiology, QIMR Berghofer Medical Research Institute, Brisbane, Australia and [14]Centre for Eye Research Australia, Melbourne University, Melbourne, Australia

*To whom correspondence should be addressed. Tel: +61 738453563; Fax: +61 733620101; Email: stuart.macgregor@qimrberghofer.edu.au

Abstract

Keratoconus is a degenerative eye condition which results from thinning of the cornea and causes vision distortion. Treatments such as ultraviolet (UV) cross-linking have proved effective for management of keratoconus when performed in early stages of the disease. The central corneal thickness (CCT) is a highly heritable endophenotype of keratoconus, and it is estimated that up to 95% of its phenotypic variance is due to genetics. Genome-wide association efforts of CCT have identified common variants (i.e. minor allele frequency (MAF) >5%). However, these studies typically ignore the large set of exonic variants whose MAF is usually low. In this study, we performed a CCT exome-wide association analysis in a sample of 1029 individuals from a population-based study in Western Australia. We identified a genome-wide significant exonic variant rs121908120 ($P = 6.63 \times 10^{-10}$) in *WNT10A*. This gene is 437 kb from a gene previously associated with CCT (*USP37*). We showed in a conditional analysis that the *WNT10A* variant completely accounts for the signal previously seen at *USP37*. We replicated our finding in independent samples from the Brisbane Adolescent Twin Study, Twin Eye Study in Tasmania and the Rotterdam Study. Further, we genotyped rs121908120 in 621 keratoconus cases and compared the frequency to a sample of 1680 unscreened controls from the Queensland Twin Registry. We found that rs121908120 increases the risk of keratoconus two times (odds ratio 2.03, $P = 5.41 \times 10^{-5}$).

Received: March 2, 2015. **Revised:** May 22, 2015. **Accepted:** June 2, 2015

Introduction

Keratoconus is a degenerative eye disease with an incidence of around 1 in 2000 in the general population (1). It is characterized by thinning and weakening of the cornea, and its symptoms range from mild astigmatism and myopia to severe vision distortion. Corneal collagen ultraviolet (UV) cross-linking is a minimally invasive and effective option for management of keratoconus at early stages (2) achieving biomechanical stabilization of the cornea and reducing (or in some cases halting) the disease progression rate. However, it is not uncommon for patients with mild or early stages of keratoconus to be misdiagnosed as cases of astigmatism or myopia and undiagnosed keratoconus can lead to corneal ectasia following laser refractive surgery (LASIK) (3).This makes it particularly important to find biomarkers that can point to keratoconus in its earliest stage.

Previous work has shown that keratoconus risk is affected by both genetic and environmental factors (4,5). Several strategies have been pursued to identify the genetic risk factors of keratoconus; however, given the low prevalence of the disease, it has been difficult to perform well-powered genomic studies (6). In contrast, genome-wide association studies (GWAS) of central corneal thickness (CCT), a highly heritable biometric trait which functions as endophenotype of keratoconus, have successfully identified 27 associated loci (7). Lu *et al.* (7) found that several of these CCT loci were also associated with keratoconus in a case–control analysis.

The identified CCT variants only explain around 8% of the variability of the trait (7). CCT is highly heritable (~90%) (8) and hence there is substantial missing heritability. One possible component of the missing heritability is low frequency variants. The published CCT GWASs to date focused primarily on common variants (i.e. minor allele frequency (MAF) > 5%). This approach ignores a large number of coding exome variants, where the MAF is usually lower. Therefore, to determine the role of low-frequency coding variants in CCT, we evaluated putative functional coding variants from the Illumina Human Exome array. We performed the association using genotype data from 1029 individuals from the Raine cohort (9). We replicated our results in two independent samples from (i) the Rotterdam Study (RS) (10) and (ii) Brisbane Adolescent Twin Study (BATS) (11,12). Further, we investigated the significant associations with CCT in a sample of 621 Australian keratoconus cases and 1680 unscreened controls.

Results

We performed an exome-wide association analysis of CCT using data from the Western Australian Pregnancy (Raine) Cohort (9). A sample of 1029 unrelated individuals of European descent and with CCT measures were used to test the association of the 43 435 exonic variants with a MAF > 0.25% passing quality control (QC). Sample characteristics are summarized in Table 1. We performed the association analysis of each variant through linear regression analysis adjusting for sex, age and the first three genetic principal components (PCs). The *genomic inflation* factor (λ) with respect to the median of χ^2-statistics was 1.006 suggesting no inflation in the test statistics due to population structure (13) (Fig. 1A.).

Figure 2 shows the results of the analysis. One single nucleotide polymorphism (SNP) reached the threshold of genome-wide significance ($P = 5.0 \times 10^{-8}$): rs121908120 in *WNT10* on chromosome 2 ($\beta = -23.84 \pm 3.92$, $P = 6.63 \times 10^{-10}$). *WNT10A* is expressed in all the ocular tissues reported in the ocular tissue database

Table 1. Descriptive statistics of the samples

	N	CCT (SD) (μm)	Age (SD) (years)	Males (%)
Raine	1029	538.2 (32.3)	20.1 (0.4)	48
BATS/TEST	147	554.5 (33.8)	22.6 (12.2)	54
RS-I	873	544.4 (33.9)	76.3 (6.7)	48
RS-II	1215	547.7 (34.2)	72.6 (5.3)	47
RS-III	2391	550.3 (33.9)	62.3 (5.8)	43

CCT, central corneal thickness; BATS/TEST, Brisbane Adolescent Twin Study/Twin Eye Study in Tasmania; RS-I, RS-II, RS-III, RS cohorts; SD, standard deviation.

(14). The SNP rs121908120 causes a missense mutation in *WNT10A* which results in a change in the amino acid 228 from phenylalanine to Isoleucine. According to SIFT (15) and PolyPhen (16), this missense mutation is deleterious (score 0) and probably damaging (score 0.994), respectively. This variant is 437 kb upstream of rs10189064 ($P = 3.11 \times 10^{-4}$) in the *USP37* gene, which was previously associated with CCT (7). These two variants are in moderate linkage disequilibrium (LD; $R^2 = 0.369$). In order to assess the extent of independent effect of these two SNPs, we performed conditional analysis (i.e. using one as covariate and testing the other and vice versa). The results are summarized in Table 2. Our results show that conditioning rs121908120 by rs10189064 does not reduce the effect ($\beta = -23.75 \pm 5.33$) of the SNP; however, the *P*-value goes down to 9.28×10^{-6} probably due to a reduction in sample size, as just 938 individuals had information on the SNP rs10189064. On the other hand, conditioning rs10189064 on the variant in *WNT10A* *removes the effect completely—the effect changes from* $\beta = -14.57 \pm 4.02$ ($P = 3.11 \times 10^{-4}$) to $\beta = 0.44 \pm 5.21$ ($P = 0.93$). This suggests that the previously identified associated SNP in *USP37* is likely due to LD confounding with the variant in *WNT10A*.

We replicated these results using data from the RS (10) (Table 2). The total sample size of this replication cohort was $n = 4479$. Although the effects were moderately smaller in these samples, the association signal for rs121908120 was clearly replicated ($\beta = -12.68 \pm 2.75$, $P = 3.87 \times 10^{-6}$). The results remained similar after conditioning on rs10189064 ($\beta = -10.92 \pm 3.7$, $P = 3.21 \times 10^{-3}$). In addition, we used available exome data from 147 participants from the BATS and Twin Eye Study in Tasmania (TEST) (11,12). However, this sample only had rs121908120 genotyped. We found that the effect in this sample replicates our finding ($\beta = -28.73 \pm 14.05$, $P = 0.04$).

Although rs121908120 is the strongest candidate SNP in the region, we used the online tool LocusTrack (17) to look for additional SNPs in high LD with rs121908120, based on the 1000 Genomes phase 3 European ancestry reference set. The only variant (rs146199923) with $r^2 = 1$ was 100 kb downstream of rs121908120, close to the *FEV* gene (Supplementary Material, Fig. S3). Examining GeneCards (18) and dbSNP, we note that rs146199923 is not a strong candidate as it lies in an intergenic region outside conserved transcription factor binding sites and DNaseI hotspots.

We also investigated the effects of exome variants in previous associated loci (7). Figure 1A displays the *P*-value distribution of SNPs within CCT known genes along with the distribution of all SNPs assessed in this study. We did not find any evidence of associated exome variants in these genes.

In addition to per SNP testing, gene-based analysis was done using the optimal unified approach SKAT-O (19). However, the approach did not alter our conclusions, as *WNT10A* ($P = 1.65 \times 10^{-10}$) was the only significant association after correction for multiple testing (Fig. 1B). The top 10 results for the gene-based

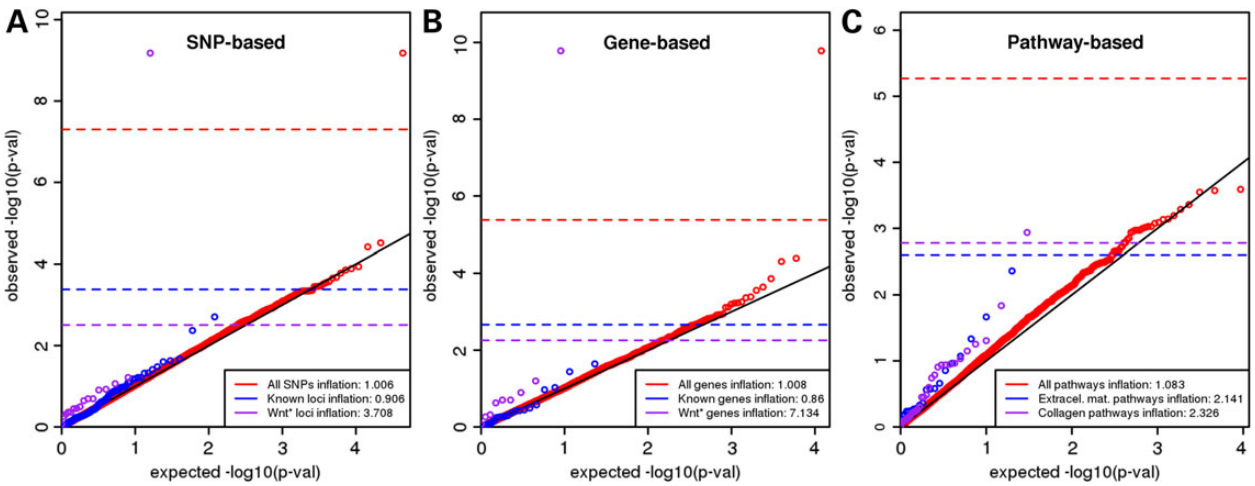

Figure 1. Quantile–Quantile plots of single SNP association (**A**), gene-based association (**B**) and pathway-based (**C**) results in the discovery cohort (Raine study). Each dot represents an observed statistic (–log 10 *P*) versus the corresponding expected statistic. The black line corresponds to the null distribution. Dotted lines show the significance threshold based on a Bonferroni correction for multiple testing.

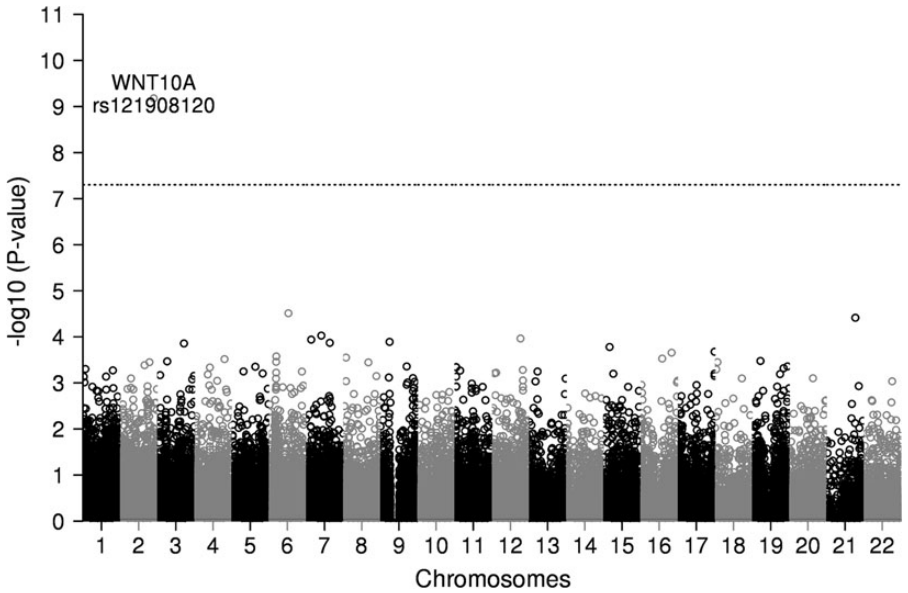

Figure 2. Manhattan plot of association results for central corneal thickness in the discovery cohort (Raine study). The plot shows –log 10-transformed *P*-values for all SNPs. The dotted horizontal line represents the threshold of genome-wide significance ($P < 5.0 \times 10^{-8}$).

test are summarized in Table 3. *WNT10A* was not associated in the gene-based analysis if rs121908120 was omitted ($P = 0.29$). Following a similar approach, we performed pathway analysis. However, in order to avoid capturing the same signal as previous experiments we removed all SNPs within the *WNT10A* gene before the analysis. Although no pathways passed the significance threshold, interestingly, the top pathway (GO:2000096, $P = 2.57 \times 10^{-4}$) was the one described as the positive regulation of the *Wnt* receptor signaling pathway (Table 4). Analyses from Lu *et al.* indicated that extracellular matrix and collagen pathways are associated with CCT (7). Analogous to inspecting variants within known associated genes, we examined the distribution of *P*-values in the collagen and extracellular matrix pathways and found an enrichment of small *P*-values for the extracellular matrix ($\lambda = 2.14$) and collagen pathways ($\lambda = 2.32$) (Fig. 1C).

Further, we genotyped rs121908120 in 621 keratoconus cases and used data from 1680 individuals from the Queensland Twin Registry, genotyped on the Illumina HumanCoreExome array, as unscreened controls. The rs121908120 MAF in keratoconus cases was 0.05 while in controls it was 0.024 translating to a 2.03-fold increase in risk (Fisher's exact test, $P = 5.41 \times 10^{-5}$).

Discussion

Our study identified a missense mutation (rs121908120) in *WNT10A* associated with CCT and keratoconus. Previous GWAS of CCT identified rs10189064 in the *USP37* gene (7), which is in moderate LD with this newly found variant rs121908120. However, the SNP in *WNT10A* has a bigger effect on CCT, and completely accounts for the signal previously seen at *USP37* in the analyzed samples.

Table 2. The results of the GWAS with CCT as outcome

SNP minor/major allele	Discovery Raine			Replication BATS/TEST		RS-I			RS-II		RS-III		RS-Meta	
	Beta ± SE	P-value	MAF	Beta ± SE	P-value	MAF	Beta ± SE	MAF	Beta ± SE	MAF	Beta ± SE	MAF	Beta ± SE	P-value
rs121908120 A/T	−23.8 ± 3.9	6.63E−10	0.030	−28.73 ± 14.1	4.10E−02	0.02	−8.76 ± 5.8	0.031	−18.46 ± 6.1	0.025	−12.18 ± 3.6	0.028	−12.68 ± 2.8	3.87E−06
rs10189064 A/G	−14.6 ± 4.0	3.11E−04	0.033	–	–	–	−4.04 ± 4.3	0.035	−12.8 ± 4.2	0.031	−6.71 ± 2.7	0.032	−7.52 ± 2.0	1.94E−04
rs121908120 a.f. rs10189064	−23.8 ± 5.3	9.28E−06	–	–	–	–	−9.27 ± 7.8	–	−11.27 ± 7.8	–	−11.46 ± 5.0	–	−10.92 ± 3.7	3.21E−03
rs10189064 a.f. rs121908120	0.44 ± 5.2	9.31E−02	–	–	–	–	0.56 ± 5.8	–	−7.99 ± 5.4	–	−0.78 ± 3.8	–	−2.34 ± 2.7	3.89E−01

Only the genome-wide significant SNP is showed (rs121908120), together with a previously known associated SNP with CCT (rs10189064). Both SNPs were conditioned for the other SNP. Beta = effect size on CCT (µm) based on the minor allele.

a.f., adjusted for; BATS/TEST, Brisbane Adolescent Twin Study/Twin Eye Study in Tasmania; MAF, minor allele frequency; RS-I, RS-II, RS-III, RS cohorts; RS-Meta, meta-analysed estimates from the three RS cohorts; SE, standard error of the beta.

Table 3. Top 10 results from the gene-based association with CCT performed using the SKAT-O approach in the Raine cohort

Gene	P-value	# SNP
WNT10A	1.65E−10	3
SH3BGR	4.07E−05	4
ANKRD6	4.94E−05	6
STEAP1B	1.38E−04	1
ATPBD4	2.28E−04	1
TAF11	2.78E−04	1
EFCAB7	4.10E−04	6
PRRG2	4.32E−04	3
CROCC	5.56E−04	1
C6orf1	5.88E−04	1

SNP, number of single nucleotide polymorphisms used for the gene-based test.

Aside from the *USP37/WNT10A* region, we did not detect association of exonic variants in or near CCT associated loci from a previous study focusing on common variation (7). This indicates that the tagged SNPs are not in LD with the previously identified common variants in those genes, or the sample size is too small to detect any association.

WNT10A belongs to the WNT gene family. This family consists of structurally related genes encoding secreted signaling molecules that have been implicated in oncogenesis and in several developmental processes, including regulation of cell fate and patterning during embryogenesis (20,21). Studies have shown that corneal endothelial cell fate is maintained by the hedgehog and WNT pathways (22,23). The corneal endothelium is responsible for maintaining the transport of fluids and solutes to the corneal stroma (which accounts for up to 90% of the total corneal thickness). A reduced endothelial cell density can have an impact on this fluid regulation leading to stromal swelling and scarring due to excess fluid (24,25), which has also been described as a complication of keratoconus (26).

A handful of studies have described structural changes in the corneal epithelium in keratoconic eyes (27–29). The corneal epithelium is an extremely thin layer composed of epithelial tissue covering the front of the cornea. Cornea epithelial cells renew continuously from limbal stem cells (LSCs) in order to maintain transparency for light transmission. A deficiency in LSCs can lead the cornea into a non-transparent or keratinized skin like epithelium (30). Molecular analysis of the Wnt signaling pathway in LSCs have shown that *WNT2*, *WNT6*, *WNT11* and *WNT16B* are over-expressed in the limbal region, while the expression of *WNT3*, *WNT7A*, *WNT7B* and *WNT10A* is upregulated in the central cornea (mature corneal epithelium) (20). Based on this, we examined the *P*-value distribution of *WNT* genes and SNPs within them. We observed that in aggregate these genes tend to have small *P*-values, although non-significant (Fig. 1A, b and Table 5). The latter suggests that might be a matter of power or fine mapping of causal variants to see significant associations within these genes.

The strong association of *WNT10A* found in keratoconus adds evidence to its possible role in cornea stability. In addition, studies indicate that mutations in *WNT10A* are also a risk factor for ectodermal dysplasia including odonto-onycho-dermal dysplasia (31,32). This syndrome is associated with abnormalities of skin as well as epidermally derived structures including, hair, teeth, nails, tongue and sweat glands. Hair including eyelashes is typically thin and sparse. Ocular features include chronic tearing, photophobia and keratitis (33).

Table 4. Top 10 results from the pathway-based association with CCT performed using the SKAT-O approach in the Raine cohort

Pathway	P-value	# SNP	Definition
GO:2000096	2.57E–04	11	Positive regulation of Wnt receptor signaling pathway
GO:0030145	2.68E–04	76	Manganese ion binding
GO:0038180	2.84E–04	19	Nerve growth factor signaling pathway
GO:1990090	4.39E–04	18	Cellular response to nerve growth factor stimulus
GO:0035249	5.18E–04	46	Synaptic transmission, glutamatergic
GO:0048406	6.45E–04	16	Nerve growth factor binding
GO:0007608	7.25E–04	175	Sensory perception of smell
GO:0003730	7.36E–04	20	mRNA 3′-UTR binding
GO:0007520	8.15E–04	53	Myoblast fusion
GO:0048172	8.41E–04	17	Regulation of short-term neuronal synaptic plasticity

SNP, number of single nucleotide polymorphisms used for the pathway-based test.

Table 5. Results of *WNT** genes available from the gene-based association with CCT performed using the SKAT-O approach in the Raine cohort

Chromosome	Position	Gene	P-value	#SNP
2	219745254	*WNT10A*	1.65E–10	3
10	102222811	*WNT8B*	0.06	1
11	75897369	*WNT11*	0.13	1
7	120969089	*WNT16*	0.2	2
7	116916685	*WNT2*	0.2	3
1	228109164	*WNT9A*	0.24	1
17	44928967	*WNT9B*	0.48	1
17	44839871	*WNT3*	0. 54	1
12	49359122	*WNT10B*	0.85	1

SNP, number of single nucleotide polymorphisms used for the gene-based test.

Other diseases that show corneal thinning as clinical feature include connective tissue disorders and osteogenesis imperfecta (34,35). Wnt signaling is essential for maintaining bone density and the homeostasis in connective tissue (36–38). Our finding adds evidence on the link of these disorders to corneal thinning.

Pathway analyses performed by Lu *et al.* (7) associated collagen and extracellular matrix pathways to CCT. Collagen fibrils are a major component of the cornea's extracellular matrix (39) and are the building blocks of the corneal stroma and Bowman's layer (40,41). Our study was underpowered to detect significant pathway associations. However, we observed smaller *P*-value in these pathways than the expected from a uniform distribution.

In conclusion, our findings indicate that *WNT10A* plays a role in the corneal thickness homeostasis and that the mutation rs121908120 is a risk factor for keratoconus. Also, this finding adds evidence to the association of *WNT10A* to odonto-onychodermal dysplasia and the link of connective tissue disorders with corneal thinning. Furthermore, suggestive results on the association of WNT genes, and the fact that they are expressed in the different ocular tissues, indicate that may be a matter of extending the sample size or a finer mapping of variants to detect their association.

Materials and Methods

Our study consisted of two phases: in the first phase, we performed exome-wide association with CCT using the Raine study sample as discovery and the RS, the BATS and TEST for replication. In the second phase, we investigated the associated variant in Australian keratoconus patients and unscreened controls from the Queensland Twin Registry (QTwin).

Raine

Sample

Recruitment of the Western Australian Pregnancy (Raine) cohort has previously been described elsewhere in detail (42). In brief, between 1989 and 1991 2900 pregnant women were recruited prior to 18-week gestation into a randomized controlled trial to evaluate the effects of repeated ultrasound in pregnancy. Children have been comprehensively phenotyped from birth to 21 years of age (average ages of one, two, three, six, eight, ten, fourteen, seventeen and twenty-one) by trained members in the Raine research team. Most of the children are of Caucasian ethnicity. Data collection included questionnaires completed by the child's primary carer and by the adolescent from age 14, physical assessments by trained assessors at all follow-up years, DNA collection from year 14 follow-up. The study was conducted with appropriate institutional ethics approval, and written informed consent was obtained from all mothers.

Phenotypes

At age 20, participants were invited for an eye study. CCT was obtained from the Pupil Center Pachymetry readout obtained by anterior segment tomography of each dilated eye taken with an Oculus Pentacam (Optikgerate GmbH, Wetzlar, Germany) (9).

Exome array

A total of 1825 participants were genotyped using the Illumina HumanExome-12v1_A array includes 247 870 markers. Approximately 90% of the markers are coding variants selected from >12 000 exome and genome sequences representing multiple ethnicities and complex traits. The remaining 10% comprises variants that have been associated with complex traits in previous GWAS, ancestry-informative markers, markers for identity-by-descent estimation, random synonymous SNPs and Human leukocyte antigen tags (43). Genotype calling was carried out in two steps. First, we called genotypes using Illumina GenomeStudio GenTrain clustering algorithm, together with the Illumina HumanExome-12v1_A product files. QC in the initial genotypes was done by excluding samples with a calling rate below 95%, and variants with a GeneTrain score <0.15, calling rate <0.95 or heterogeneity excess <−0.3 or >0.2. We performed PC analysis, and excluded samples that were above 6 SD from the centroid of the 1000 Genomes (44) European population (GBR + CEU + FIN) PC1 and PC2. In the second step we used zCall (45) with the

default parameters to improve calling of rare variants on the remaining samples. We excluded variants with calling rate <99%, or which deviate from Hardy–Weinberg equilibrium (HWE), $P < 10^{-6}$, resulting in 235 619 variants and 1563 individuals passing QC.

Statistical analysis

Among the genotyped individuals passing QC, 1029 unrelated individuals (proportion of identity by descent <0.2) counted with CCT phenotype data. To ensure that the variants tested had at least five copies of the minor allele, we restricted the analyses to just those variants with a MAF > 0.25% (i.e. 43 435 SNPs). Single SNP-based analysis was carried out using linear regression in plink (46,47) and adjusting by sex, age and the first three PCs. The genotype cluster plot for the top associated variant rs121908120 is displayed in Supplementary Material, Figure S1.

Gene and pathway-based association analyses were performed using SKAT-O (19), which performs association test of SNP sets and optimally combines the burden test and the non-burden sequence kernel association test (SKAT). Gene-based SNP sets were created using the SNP-gene annotation file from the Illumina Human-Exome bead-chip. Pathways were based on the Gene Ontology database (48). Pathway-based SNP sets were composed by the SNPs within the genes involved in each particular pathway.

We performed conditional analysis of rs10189064 and rs121908120 using Plink (46). Given that the Illumina HumanExome-12v1_A does not contain rs10189064 among the tagged SNPs, we extracted the rs10189064 genotype from 938 individuals that were also genotyped in the Human660W-Quad bead chip for previous experiments. Genotyping and QC details for the Human660W-Quad bead chip in the Raine sample are described elsewhere (7). In brief 1593 individuals were genotyped in 2009 using the Human660W-Quad bead chip, as part of QC, the data were filtered by SNP call rate <0.95, a HWE, $P < 10^{-6}$ and a MAF >1%.To exclude population outliers, a principal component analysis (PCA) was carried out using SNPs with genotyping rate >0.98.

The RS

Samples

The RS is a population-based study held in Rotterdam, the Netherlands (10). It consists of three cohorts. The original cohort, RS-I, started in 1990 and includes 7983 subjects aged 55 years and older. The second cohort, RS-II, was added in 2000 and includes 3011 subjects aged 55 years and older. The last cohort, RS-III, includes 3932 subjects of 45 years of age and older and started in 2006. The RS has been approved by the Medical Ethics Committee of the Erasmus MC and by the Ministry of Health, Welfare and Sport of the Netherlands, implementing the 'Wet Bevolkingsonderzoek: ERGO (Population Studies Act: Rotterdam Study)'. All participants provided written informed consent to participate in the study and to obtain information from their treating physicians.

Phenotype

CCT was measured using ultrasound pachymetry (Allergan Humphrey 850, Carl Zeiss Meditec, Dublin, CA, USA; subset of RS-I), and using a non-contact biometer (Lenstar LS900, Haag-Streit, Köniz, Switzerland; subset of RS-I, RS-II and RS-III).

Genotyping and association

Genotyping of SNPs was performed using the Illumina Infinium II HumanHap550 array (RS-I), the Illumina Infinium HumanHap 550-Duo array (RS-I, RS-II) and the Illumina Infinium Human 610-Quad array (RS-I, RS-III). Samples with low call rate (<97.5%), with excess autosomal heterozygosity (>0.336), or with sex-mismatch were excluded, as were outliers identified by the identity-by-state clustering analysis (outliers were defined as being >3 SD from population mean or having identity-by-state probabilities >97%). A set of genotyped input SNPs with call rate >98%, MAF >0.1% and Hardy–Weinberg P-value $>10^{-6}$ was used for imputation. The Markov Chain Haplotyping (MACH) package version 1.0 software (49) (Rotterdam, The Netherlands; imputed to plus strand of NCBI build 37, 1000 Genomes phase I version 3) and minimac version 2012.8.6 was used for the imputation. Number of samples remained for RS are summarized in Table 1. Imputation quality (r^2) for rs121908120 was RSI = 0.61, RSII = 0.57 and RSIII = 0.63 and for rs10189064 r^2 was above 0.99 in the three studies. Association analyses of rs121908120 and rs10189064 variants with CCT were performed using the ProbABEL package (50) using age, sex, the first five PCs and the technique of measurement (the latter only for RS-I) as covariates.

BATS and TEST

Samples

Methodologies and recruitment of participants from the BATS and TEST are described elsewhere (11,12).

Phenotype

CCT was measured in this cohort using ultrasound pachymetry and recorded for both eyes. Measurements were performed using a Tomey SP 2000 (Tomey Corp., Nagoya, Japan).

Genotyping and association

Genotyping of 147 individuals from BATS and TEST with eye phenotype was performed using the Illumina HumanCoreExome array. Samples and SNPs with low call rate (<98%) were excluded, as well as variants with MAF <0.1% and Hardy–Weinberg P-value $>10^{-6}$. Association was performed using Merlin which effectively accounts for family structure (51). Age, sex and the first three PCs were used as covariates.

Queensland Twin Registry

Samples

Methodologies and recruitment of the Queensland Twin Registry are described elsewhere (REF above). The unscreened controls for the keratoconus samples were a subset of the BATS and TEST projects. These controls were family members from BATS and TEST projects, selected to be unrelated to the 147 BATS and TEST individuals included in the CCT scan. The unscreened controls were pruned to remove related individuals (typically both parents of a twin pair were used as controls).

Genotyping

Genotyping was carried out as described for the BATS and TEST CCT samples.

Keratoconus cases

Sample

Australian participants with keratoconus ($n = 621$) were ascertained through the Department of Ophthalmology of Flinders Medical Centre, Adelaide, Australia; private optometry practices in Adelaide and Melbourne, Australia; the Royal Victorian Eye and Ear Hospital, Melbourne, Australia; and by Australia-wide

mail out to members of Keratoconus Australia, a community-based support group for patients.

Phenotypes

The diagnosis of keratoconus was based on clinical examination and videokeratography pattern analysis. Clinical examination included slit lamp biomicroscopy, cycloplegic retinoscopy and fundus evaluations. Slit lamp biomicroscopy was used to identify stromal corneal thinning, Vogt's striae or a Fleischer ring. A retinoscopic examination was performed with a fully dilated pupil to determine the presence or absence of retroillumination signs of keratoconus, such as the oil droplet sign and scissoring of the red reflex. Videokeratography evaluation was performed on each eye by topographic modeling. Patients were considered as having keratoconus if they had at least one clinical sign of the disease and by confirmatory videokeratography map with an asymmetric bowtie pattern with skewed radial axis above and below the horizontal meridian (AB/SRAX). A history of penetrating keratoplasty performed because of keratoconus was also sufficient for inclusion.

Genotyping

Genotyping of rs121908120 in 621 individuals was completed using a pre-designed Taqman assay (Life Technologies), amplified in SensiFAST Probe No-ROX master mix (Bioline) on a LightCycler480 Real-time PCR Machine (Roche), according to manufacturer's protocol. The genotyping cluster plot for rs121908120 genotyping is displayed in Supplementary Material, Figure S2.

Supplementary Material

Supplementary Material is available at *HMG* online.

Acknowledgements

We acknowledge the contribution of Ada Hooghart, Corina Brussee, Riet Bernaerts-Biskop, Patricia van Hilten, Pascal Arp, Jeanette Vergeer and Maarten Kooijman. We thank Pascal Arp, Mila Jhamai, Marijn Verkerk, Lizbeth Herrera and Marjolein Peters for their help in creating the GWAS database, and Karol Estrada and Maksim V. Struchalin for their support in creation and analysis of imputed data. The authors are grateful to the study participants, the staff from the Rotterdam Study and the participating general practitioners and pharmacists. A full set of summary association statistics are available at gump.qimr.edu.au/general/gabrieC/CCT. The authors thank the Raine Study participants and their families and research staff from the Lions Eye Institute and the Raine Study Team.

Conflict of Interest statement. The authors declare that there are no conflicts of interest.

Funding

G.C.P. thanks the University of Queensland and QIMR Berghofer Medical Research Institute for scholarship support. The Rotterdam Study was supported by the Netherlands Organisation of Scientific Research (NWO; 91111025); Erasmus Medical Center and Erasmus University, Rotterdam, The Netherlands; Netherlands Organization for Health Research and Development (ZonMw); UitZicht; the Research Institute for Diseases in the Elderly; the Ministry of Education, Culture and Science; the Ministry for Health, Welfare and Sports; the European Commission (DG XII); the Municipality of Rotterdam; the Netherlands Genomics Initiative/NWO; Center for Medical Systems Biology of NGI; Stichting Lijf en Leven; Stichting Oogfonds Nederland; Landelijke Stichting voor Blinden en Slechtzienden; Algemene Nederlandse Vereniging ter Voorkoming van Blindheid; Medical Workshop; Heidelberg Engineering; and Topcon Europe BV. H.S. is supported by the NWO Graduate Programme 2010 BOO (022.002.023) and by Prins Bernhard Cultuurfonds (Cultuurfondsbeurs from Jan de Ruijsscher/Pia Huisman fonds). The generation and management of GWAS genotype data for the Rotterdam Study is supported by the Netherlands Organisation of Scientific Research NWO Investments (nr. 175.010.2005.011, 911-03-012). This study is funded by the Research Institute for Diseases in the Elderly (014-93-015; RIDE2), the Netherlands Genomics Initiative (NGI)/Netherlands Organisation for Scientific Research (NWO) project nr. 050-060-810. The keratoconus cohort was supported by the Ophthalmic Research Institute of Australia and NHMRC Centre for Research Excellence grant (1023911). K.P.B. and J.E.C. are supported by NHMRC Senior and Practitioner Research Fellowships, respectively. S.E.M.L. thanks the Menzies Institute for Medical Research and the Moonah Naval Club for scholarship support. S.M. is supported by an Australian Research Council Future Fellowship. D.A.M thanks the Australian National Health and Medical Research Council Project Grants 1021105, Channel 7 Telethon Trust, Ophthalmic Research Institute of Australia (ORIA), University of Western Australia (UWA), The Telethon Kids Institute, Raine Medical Research Foundation, Women's and Infants' Research Foundation, The UWA Faculty of Medicine, Curtin University, Edith Cowan University, the Australian Foundation for the Prevention of Blindness.

References

1. Rabinowitz, Y.S. (1998) Keratoconus. *Surv. Ophthalmol.*, **42**, 297–319.
2. Bikbov, M.M., Bikbova, G.M. and Khabibullin, A.F. (2011) Corneal collagen cross-linking in keratoconus management. *Vestn. Oftalm.*, **127**, 21–25.
3. Randleman, J.B., Russell, B., Ward, M.A., Thompson, K.P. and Stulting, R.D. (2003) Risk factors and prognosis for corneal ectasia after LASIK. *Ophthalmology*, **110**, 267–275.
4. Burdon, K.P. and Vincent, A.L. (2013) Insights into keratoconus from a genetic perspective. *Clin Exp Optom.*, **96**, 146–154.
5. Davidson, A.E., Hayes, S., Hardcastle, A.J. and Tuft, S.J. (2014) The pathogenesis of keratoconus. *Eye*, **28**, 189–195.
6. Li, X., Bykhovskaya, Y., Haritunians, T., Siscovick, D., Aldave, A., Szczotka-Flynn, L., Iyengar, S.K., Rotter, J.I., Taylor, K.D. and Rabinowitz, Y.S. (2012) A genome-wide association study identifies a potential novel gene locus for keratoconus, one of the commonest causes for corneal transplantation in developed countries. *Hum. Mol. Genet.*, **21**, 421–429.
7. Lu, Y., Vitart, V., Burdon, K.P., Khor, C.C., Bykhovskaya, Y., Mirshahi, A., Hewitt, A.W., Koehn, D., Hysi, P.G., Ramdas, W.D. *et al.* (2013) Genome-wide association analyses identify multiple loci associated with central corneal thickness and keratoconus. *Nat. Genet.*, **45**, 155–163.
8. Dimasi, D.P., Burdon, K.P. and Craig, J.E. (2010) The genetics of central corneal thickness. *Brit. J. Ophthalmol.*, **94**, 971–976.
9. Yazar, S., Forward, H., McKnight, C.M., Tan, A., Soloshenko, A., Oates, S.K., Ang, W., Sherwin, J.C., Wood, D., Mountain, J.A. *et al.* (2013) Raine eye health study: design, methodology and baseline prevalence of ophthalmic disease in a birth-cohort study of young adults. *Ophthalmic Genet.*, **34**, 199–208.

10. Hofman, A., Darwish Murad, S., van Duijn, C.M., Franco, O.H., Goedegebure, A., Ikram, M.A., Klaver, C.C., Nijsten, T.E., Peeters, R.P., Stricker, B.H. *et al.* (2013) The Rotterdam Study: 2014 objectives and design update. *Eur. J. Epidemiol.*, **28**, 889–926.
11. Wright, M.J. and Martin, N.G. (2011) Brisbane Adolescent Twin Study: outline of study methods and research projects. *Aust. J. Psychol.*, **56**, 65–78.
12. Mackey, D.A., Mackinnon, J.R., Brown, S.A., Kearns, L.S., Ruddle, J.B., Sanfilippo, P.G., Sun, C., Hammond, C.J., Young, T.L., Martin, N.G. *et al.* (2009) Twins eye study in Tasmania (TEST): rationale and methodology to recruit and examine twins. *Twin Res. Hum. Genet.*, **12**, 441–454.
13. Yang, J., Weedon, M.N., Purcell, S., Lettre, G., Estrada, K., Willer, C.J., Smith, A.V., Ingelsson, E., O'Connell, J.R., Mangino, M. *et al.* (2011) Genomic inflation factors under polygenic inheritance. *Eur. J. Hum. Genet.*, **19**, 807–812.
14. Wagner, A.H., Anand, V.N., Wang, W.H., Chatterton, J.E., Sun, D., Shepard, A.R., Jacobson, N., Pang, I.H., Deluca, A.P., Casavant, T.L. *et al.* (2013) Exon-level expression profiling of ocular tissues. *Exp. Eye Res.*, **111**, 105–111.
15. Ng, P.C. and Henikoff, S. (2003) SIFT: Predicting amino acid changes that affect protein function. *Nucleic Acids Res.*, **31**, 3812–3814.
16. Adzhubei, I.A., Schmidt, S., Peshkin, L., Ramensky, V.E., Gerasimova, A., Bork, P., Kondrashov, A.S. and Sunyaev, S.R. (2010) A method and server for predicting damaging missense mutations. *Nat. Methods*, **7**, 248–249.
17. Cuellar-Partida, G., Renteria, M.E. and MacGregor, S. (2015) LocusTrack: integrated visualization of GWAS results and genomic annotation. *Source Code Biol. Med.*, **10**, 1.
18. Safran, M., Dalah, I., Alexander, J., Rosen, N., Iny Stein, T., Shmoish, M., Nativ, N., Bahir, I., Doniger, T., Krug, H. *et al.* (2010) GeneCards Version 3: the human gene integrator. *Database*, **2010**, baq020.
19. Lee, S., Emond, M.J., Bamshad, M.J., Barnes, K.C., Rieder, M.J. and Nickerson, D.A., NHLBI GO Exome Sequencing Project—ESP Lung Project Team, Christiani, D.C., Wurfel, M.M. and Lin, X. (2012) Optimal unified approach for rare-variant association testing with application to small-sample case–control whole-exome sequencing studies. *Am. J. Hum. Genet.*, **91**, 224–237.
20. Nakatsu, M.N., Ding, Z., Ng, M.Y., Truong, T.T., Yu, F. and Deng, S.X. (2011) Wnt/beta-catenin signaling regulates proliferation of human cornea epithelial stem/progenitor cells. *Invest. Ophthalmol. Vis. Sci.*, **52**, 4734–4741.
21. Nusse, R. (2008) Wnt signaling and stem cell control. *Cell Res.*, **18**, 523–527.
22. Ouyang, H., Xue, Y., Lin, Y., Zhang, X., Xi, L., Patel, S., Cai, H., Luo, J., Zhang, M., Zhang, M. *et al.* (2014) WNT7A and PAX6 define corneal epithelium homeostasis and pathogenesis. *Nature*, **511**, 358–361.
23. Hirata-Tominaga, K., Nakamura, T., Okumura, N., Kawasaki, S., Kay, E.P., Barrandon, Y., Koizumi, N. and Kinoshita, S. (2013) Corneal endothelial cell fate is maintained by LGR5 through the regulation of hedgehog and Wnt pathway. *Stem Cells*, **31**, 1396–1407.
24. Meek, K.M., Leonard, D.W., Connon, C.J., Dennis, S. and Khan, S. (2003) Transparency, swelling and scarring in the corneal stroma. *Eye*, **17**, 927–936.
25. Srinivas, S.P. (2010) Dynamic regulation of barrier integrity of the corneal endothelium. *Optom. Vis. Sci.*, **87**, E239–E254.
26. Fan Gaskin, J.C., Patel, D.V. and McGhee, C.N. (2014) Acute corneal hydrops in keratoconus—new perspectives. *Am. J. Ophthalmol.*, **157**, 921–928.
27. Hiratsuka, Y., Nakayasu, K. and Kanai, A. (2000) Secondary keratoconus with corneal epithelial iron ring similar to Fleischer's ring. *Jpn J. Ophthalmol.*, **44**, 381–386.
28. Reinstein, D.Z., Archer, T.J. and Gobbe, M. (2009) Corneal epithelial thickness profile in the diagnosis of keratoconus. *J. Refract. Surg.*, **25**, 604–610.
29. Zhou, W. and Stojanovic, A. (2014) Comparison of corneal epithelial and stromal thickness distributions between eyes with keratoconus and healthy eyes with corneal astigmatism >/= 2.0 D. *PLoS One*, **9**, e85994.
30. Sejpal, K., Bakhtiari, P. and Deng, S.X. (2013) Presentation, diagnosis and management of limbal stem cell deficiency. *Middle East Afr. J. Ophthalmol.*, **20**, 5–10.
31. Kantaputra, P., Kaewgahya, M., Jotikasthira, D. and Kantaputra, W. (2014) Tricho-odonto-onycho-dermal dysplasia and WNT10A mutations. *Am. J. Med. Genet. A*, **164A**, 1041–1048.
32. Nawaz, S., Klar, J., Wajid, M., Aslam, M., Tariq, M., Schuster, J., Baig, S.M. and Dahl, N. (2009) WNT10A missense mutation associated with a complete odonto-onycho-dermal dysplasia syndrome. *Eur. J. Hum. Genet.*, **17**, 1600–1605.
33. Zirbel, G.M., Ruttum, M.S., Post, A.C. and Esterly, N.B. (1995) Odonto-onycho-dermal dysplasia. *Brit. J. Dermatol.*, **133**, 797–800.
34. Evereklioglu, C., Madenci, E., Bayazit, Y.A., Yilmaz, K., Balat, A. and Bekir, N.A. (2002) Central corneal thickness is lower in osteogenesis imperfecta and negatively correlates with the presence of blue sclera. *Ophthalmic Physiol. Opt.*, **22**, 511–515.
35. Pedersen, U. and Bramsen, T. (1984) Central corneal thickness in osteogenesis imperfecta and otosclerosis. *ORL J. Otorhinolaryngol. Relat. Spec.*, **46**, 38–41.
36. Cisternas, P., Vio, C.P. and Inestrosa, N.C. (2014) Role of Wnt signaling in tissue fibrosis, lessons from skeletal muscle and kidney. *Curr. Mol. Med.*, **14**, 510–522.
37. Lloyd, S.A., Loiselle, A.E., Zhang, Y. and Donahue, H.J. (2014) Shifting paradigms on the role of connexin43 in the skeletal response to mechanical load. *J. Bone Miner. Res.*, **29**, 275–286.
38. Xie, J., Tong, P.J. and Xiao, L.W. (2013) Progress on Wnt/beta-catenin signal pathway regulating the cartilage metabolism in osteonecrosis. *Zhongguo gu Shang. China J. Orthop. Traumatol.*, **26**, 613–616.
39. Michelacci, Y.M. (2003) Collagens and proteoglycans of the corneal extracellular matrix. *Braz. J. Med. Biol. Res.*, **36**, 1037–1046.
40. Dua, H.S., Faraj, L.A., Said, D.G., Gray, T. and Lowe, J. (2013) Human corneal anatomy redefined: a novel pre-Descemet's layer (Dua's layer). *Ophthalmology*, **120**, 1778–1785.
41. Hayashi, S., Osawa, T. and Tohyama, K. (2002) Comparative observations on corneas, with special reference to Bowman's layer and Descemet's membrane in mammals and amphibians. *J. Morphol.*, **254**, 247–258.
42. McKnight, C.M., Newnham, J.P., Stanley, F.J., Mountain, J.A., Landau, L.I., Beilin, L.J., Puddey, I.B., Pennell, C.E. and Mackey, D.A. (2012) Birth of a cohort—the first 20 years of the Raine study. *Med. J. Austr.*, **197**, 608–610.
43. Huyghe, J.R., Jackson, A.U., Fogarty, M.P., Buchkovich, M.L., Stancakova, A., Stringham, H.M., Sim, X., Yang, L., Fuchsberger, C., Cederberg, H. *et al.* (2013) Exome array analysis identifies new loci and low-frequency variants influencing insulin processing and secretion. *Nat. Genet.*, **45**, 197–201.
44. Genomes Project, C., Abecasis, G.R., Auton, A., Brooks, L.D., DePristo, M.A., Durbin, R.M., Handsaker, R.E., Kang, H.M., Marth, G.T. and McVean, G.A. (2012) An integrated map of genetic variation from 1,092 human genomes. *Nature*, **491**, 56–65.
45. Goldstein, J.I., Crenshaw, A., Carey, J., Grant, G.B., Maguire, J., Fromer, M., O'Dushlaine, C., Moran, J.L., Chambert, K., Stevens, C. *et al.* (2012) zCall: a rare variant caller for array-

based genotyping: genetics and population analysis. *Bioinformatics*, **28**, 2543–2545.
46. Purcell, S., Neale, B., Todd-Brown, K., Thomas, L., Ferreira, M.A., Bender, D., Maller, J., Sklar, P., de Bakker, P.I., Daly, M.J. *et al.* (2007) PLINK: a tool set for whole-genome association and population-based linkage analyses. *Am. J. Hum. Genet.*, **81**, 559–575.
47. Chang, C.C., Chow, C.C., Tellier, L.C.A.M., Vattikuti, S., Purcell, S.M. and Lee, J.J. (2015) Second-generation PLINK: rising to the challenge of larger and richer datasets. *GigaScience*, **4**, 7.
48. Harris, M.A., Clark, J., Ireland, A., Lomax, J., Ashburner, M., Foulger, R., Eilbeck, K., Lewis, S., Marshall, B., Mungall, C. *et al.* (2004) The Gene Ontology (GO) database and informatics resource. *Nucleic Acids Res.*, **32**, D258–D261.
49. Li, Y., Willer, C.J., Ding, J., Scheet, P. and Abecasis, G.R. (2010) MaCH: using sequence and genotype data to estimate haplotypes and unobserved genotypes. *Genet. Epidemiol.*, **34**, 816–834.
50. Aulchenko, Y.S., Struchalin, M.V. and van Duijn, C.M. (2010) ProbABEL package for genome-wide association analysis of imputed data. *BMC Bioinformatics*, **11**, 134.
51. Abecasis, G.R., Cherny, S.S., Cookson, W.O. and Cardon, L.R. (2002) Merlin—rapid analysis of dense genetic maps using sparse gene flow trees. *Nat. Genet.*, **30**, 97–101.